Bull. Mater. Sci., Vol. 32, No. 4, August 2009, pp. 443–449. © Indian Academy of Sciences.

Synthesis, structural and ferromagnetic properties of $La_{1-x}K_xMnO_3$ ($0{\cdot}0 \leq x \leq 0{\cdot}25$) phases by solution combustion method

C SHIVAKUMARA* and MANJUNATH B BELLAKKI

Solid State and Structural Chemistry Unit, Indian Institute of Science, Bangalore 560 012, India

MS received 18 August 2008; revised 5 September 2009

Abstract. **We describe the solution combustion synthesis and characterization of $La_{1-x}K_xMnO_3$ ($0{\cdot}0 \leq x \leq 0{\cdot}25$) perovskite phases, which is a low temperature initiated, rapid route to prepare metal oxides. As-synthesized compounds are amorphous in nature; crystallinity was observed on heating at 800°C for 5 min. Structural parameters were determined by the Rietveld refinement method using powder XRD data. Parent $LaMnO_3$ compound crystallizes in the orthorhombic structure (space group *Pbnm*, No. 62). Potassium substituted compounds were crystallized with rhombohedral symmetry (space group *R–3c*, No. 167). The ratio of the Mn^{3+}/Mn^{4+} was determined by the iodometric titration. The Fourier transform infrared spectrum (FT–IR) shows two absorption bands for Mn–O stretching vibration (ν_s mode), Mn–O–Mn deformation vibration (ν_b mode) around 600 cm^{-1} and 400 cm^{-1} for the compositions, $x = 0{\cdot}0$, $0{\cdot}05$ and $0{\cdot}10$. Four-probe electrical resistivity measurements reveal a composition controlled metal to insulator transition ($T_{M–I}$), the maximum $T_{M–I}$ was observed for the composition $La_{0{\cdot}85}K_{0{\cdot}15}MnO_3$ at 287 K. Room temperature vibrating sample magnetometer data indicate that for the composition up to $x = 0{\cdot}10$, the compounds are paramagnetic whereas composition with $x = 0{\cdot}15$, $0{\cdot}20$ and $0{\cdot}25$ show magnetic moments of 27, 29 and 30 emu/g, respectively.**

Keywords. **Perovskite; XRD; crystal structure; electrical properties; magnetic materials.**

1. Introduction

Alkaline earth metal ions (Ca^{2+}, Sr^{2+}, Ba^{2+}, and Pb^{2+}) substitution for La^{3+} ion in $LaMnO_3$ inducing ferromagnetic metallic property is known for a long time (Jonker and Van Santen 1950). The renewed interest on doped-manganites came from the observation of a high colossal magnetoresistive (CMR) effect, which triggered the attention of the scientific community. Observation of colossal magnetoresistance (CMR) in $La_{1-x}Ba_xMnO_3$ thin films has created new interest in these materials (von Helmolt *et al* 1993). New phenomena, viz. charge, spin, and orbital ordering has been discovered in these perovskite-based rare earth manganites (Rao *et al* 1996; Raveau *et al* 1998; Rao 2000). The ratio of Mn^{3+} and Mn^{4+} is an important factor to show insulator to metal (I–M) transition and magnetic phase transition in manganites. It is possible to achieve an equal amount of hole doping with half the number of the monovalent ions, because for the same amount of aliovalent dopant the hole density is twice that of the divalent ion doping. Monovalent ion-doped rare earth manganites of the general formula, $Ln_{1-x}A_xMnO_3$ (Ln = La, Pr, Nd; A = Na, K, Rb), provide another series of oxides to study the physical phenomena of insulator-to-metal transition and colossal magnetoresistance (Itoh *et al* 1995; Shimura *et al* 1996; Chen and de Lozanne 1997; Ng-Lee *et al* 1997; Sahana *et al* 1997; Singh *et al* 1998). Alkali metal ion doped lanthanum manganites have been prepared by the conventional ceramic methods (Itoh *et al* 1995; Shimura *et al* 1996), alkali-flux method (Singh *et al* 1998; Shivakumara *et al* 2004) and fused salt electrolysis (McCarroll *et al* 1999).

Solution combustion method offers an advantage over the other conventional methods. It is a low-temperature initiated exothermic and self-propagating process. Patil *et al* (1997) reviewed synthesis of various oxide materials by the combustion reactions of redox mixtures containing stoichiometric amounts of respective metal nitrates (oxidizers) and fuels. Employing the solution combustion method, a wide range of technologically useful oxides having magnetic, dielectric, electrical, mechanical, luminescent, optical properties and divalent ion doped lanthanum manganites (Aruna *et al* 1997) were prepared. Recently nanocrystalline $La_{1-x}Ba_xMnO_3$ (Nagabhushana *et al* 2005), $La_{1-x}Sr_xMnO_3$ (Nagabhushana *et al* 2006) and sodium doped $LaMnO_3$ by combustion (Shivakumara *et al* 2007) and the sol gel and propellant method (Malavasi *et al* 2003) were reported. In this paper we report for the first time, rapid synthesis, structure, electrical and magnetic properties of potassium substituted lanthanum manganites perovskite phases by the solution combustion

*Author for correspondence (shiva@sscu.iisc.ernet.in)

method at relatively low temperature and shorter duration.

2. Experimental

$La_{1-x}K_xMnO_3$ ($0{\cdot}00 \le x \le 0{\cdot}25$) perovskite phases were synthesized by the rapid solution combustion method using oxyldihydrazide (ODH) as a fuel. The detailed procedure for calculating the metal nitrates to fuel ratio has been described elsewhere (Patil 1993; Patil *et al* 1997). Stoichiometric amounts of $La(NO_3)_3$ (obtained by dissolving the requisite amount of preheated La_2O_3 at 800°C), KNO_3 and $Mn(NO_3)_2{\cdot}4H_2O$ were dissolved in a minimum amount of water in a pyrex dish. Calculated amounts of the fuel ODH were added. The ODH dissolved and formed a clear solution which was introduced into a muffle furnace preheated to 400°C. The mixture boiled, followed by frothing and ignited with evolution of large amount of gases. The flame persisted for about a minute leaving behind a residual black coloured fine powder. Assuming complete combustion, the general equation for the formation of samples can be proposed as follows

$$(1-x)La(NO_3)_3(aq) + xK(NO_3)(aq) + Mn(NO_3)_2(aq) + C_2H_6N_4O_2(aq) \rightarrow La_{1-x}K_xMnO_3(S) + CO_2(g) + H_2O(g) + N_2(g).$$

All the samples were characterized by powder X-ray diffraction (XRD) using a Philips X'pert Pro diffractometer with CuKα (λ = 1·5418 Å) using a graphite monochromator to filter the K_β lines. The resulting powder was X-ray amorphous in nature. To obtain crystallinity, this powder was heated at 800°C for 2 h. For Rietveld refinement, data were collected at a scan rate of 1°/min with a 0·02° step size for 2θ from 10° to 80°. The data were refined using the Foolproof Suite-2000 version. Infrared spectra for calcined samples were recorded on a Perkin-Elmer FT–IR Spectrometer spectrum 1000 from 300–4000 cm^{-1}. Electrical resistivity measurement was carried out on the sintered pellets at 800°C for 12 h by a four-probe method in the temperature range from 300–12 K. Room temperature magnetic measurements were carried out using a vibrating sample magnetometer (VSM; Lake Shore).

2.1 *Determination of Mn^{3+}/Mn^{4+} concentration*

The ratio of the Mn^{3+}/Mn^{4+} concentration was determined by iodometric titration for the sintered compounds (Singh *et al* 1998). Typically, about 50 mg of the compound was dissolved in 10 ml of 1 : 1 HCl containing about 1 g of solid potassium iodide. Liberated iodine was titrated against standard sodium thiosulphate (0·05 N) solution using starch as an indicator.

3. Results and discussion

Figure 1 shows the powder X-ray diffraction (XRD) patterns for the typical $La_{0{\cdot}85}K_{0{\cdot}15}MnO_3$ compound (a) as synthesized and calcined at 800°C from 5 min to 2 h (figures 1(b)–(g)). The as synthesized compound is amorphous in nature. However, the fact that a crystalline perovskite oxide is formed within 5 min of calcination at 800°C, shows that the amorphous product contains metal oxides, probably in the nanoparticulate form. The question arises as to why the as-synthesized product is amorphous in nature. In this system, it is necessary to moderate the flame temperature in order to suppress the loss of potassium ions at the cost of crystallinity. The exothermicity of the combustion reaction depends on the oxidizer (O) to fuel (F) ratio and the maximum is observed when O/F = 1. Here, we have controlled the exothermicity of the reaction by making it fuel lean i.e. by adding excess nitrate source (oxidizer). As a result of less exothermic reaction the products formed are amorphous and the composition is nearer to nominal as the potassium ion evaporation is fully controlled. The XRD pattern in the product oxide could be indexed in rhombohedral symmetry (see figure 2(b) having the lattice parameters, a = 5·511(4) Å and c = 13·391(5) Å) (hexagonal

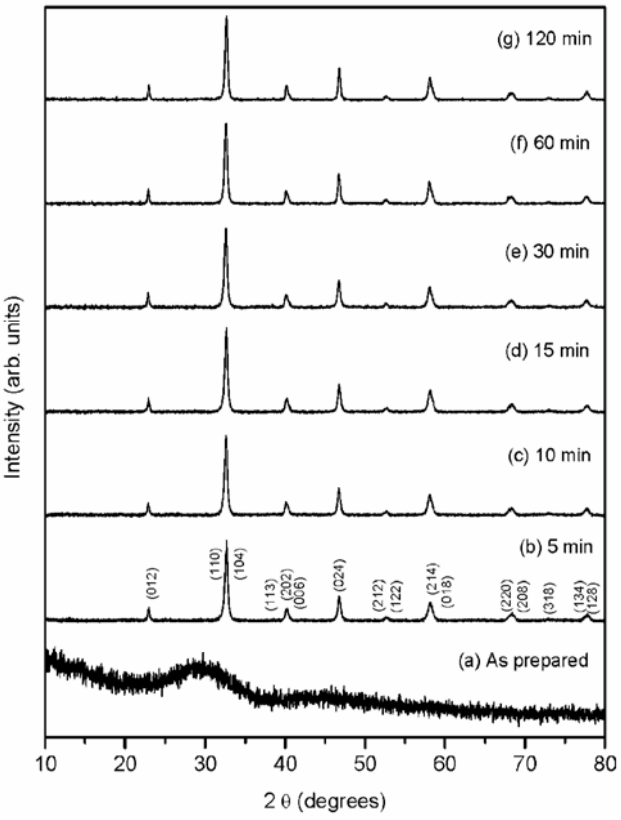

Figure 1. Powder X-ray diffraction patterns of $La_{0{\cdot}85}K_{0{\cdot}15}MnO_3$ (a) as prepared and (b–g) calcined at 800°C from 5 min to 2 h.

setting) with space group *R*–3*c* (No. 167). There is no structural change with increasing calcination time. The average crystallite size from XRD data was calculated using the Debye–Scherrer formula (Scherrer 1918). The average crystallite sizes were found to be in the range of 25–34 nm.

We synthesized a series of potassium substituted lanthanum manganites having the general formula, $La_{1-x}K_xMnO_3$ ($0{\cdot}00 \le x \le 0{\cdot}25$), as aliovalent doping of La^{3+} by K^+ is expected to generate twice the Mn^{4+} content when compared to the better known Sr^{2+} doped system (Nagabhushana *et al* 2006). In figure 2, we have shown the powder XRD patterns of all the compounds sintered at 800°C for 12 h. The parent $LaMnO_3$ compound crystallizes in the orthorhombic structure with space group *Pbnm* (No. 62), and the indexed diffraction pattern is shown in figure 2(a). The potassium substituted compounds crystallize in the rhombohedral structure (hexagonal setting) with space group *R*–3*c* (No. 167), indexed powder XRD pattern is given for the composition $La_{0{\cdot}95}K_{0{\cdot}05}MnO_3$ in figure 2(b). As the potassium content increased from $x = 0{\cdot}05$ to 0·25, the rhombohedral phase transfers to cubic like symmetry (figure 2(b–f)). The splitting of the main (1 1 0) and (1 0 4) lines decreases and seems to merge into one line. For the composition, $x = 0{\cdot}25$ from figure 2(f), we observed evolution of secondary layered phase of K_xMnO_2 (5%) at 2θ, 12·5 and 25. In the rhombohedral structure, lanthanum and potassium ions have a 12-coordination, the ionic radii (Shannon 1976) of lanthanum, $r^{3+}_{La} = 1{\cdot}36$ Å and potassium, $r^{+}_{K} = 1{\cdot}64$ Å, respectively. Due to the differences in size, it can be revealed that up to 20% of K- can be substituted for La-site in the $LaMnO_3$ system. The structural parameters for all the phases were obtained from the Rietveld refinement method. In table 1, we summarized refined structural parameters for all the compositions. Typical, observed, calculated and the difference XRD pattern for $La_{0{\cdot}85}K_{0{\cdot}15}MnO_3$ compound is given in figure 3. There is a good agreement between observed and calculated patterns. In figure 4, we have shown the model crystal structures of (a) parent $LaMnO_3$ in the orthorhombic and (b) $La_{0{\cdot}85}K_{0{\cdot}15}MnO_3$ compound in the rhombohedral structures.

Wet chemical analysis results reveal that Mn^{4+} content increases with increasing potassium content from 15–46%. Parent $LaMnO_3$ sample showed minimum 15% of Mn^{4+} content, whereas 5%, 10%, 15%, 20%, and 25% potassium-substituted compounds showed 26%, 28%, 32%, 42%, and 46% of Mn^{4+} content, respectively. Contrary to expectations the compositions with a low *x* value are relatively richer in Mn^{4+}, and compositions with higher *x* values are relatively poorer than what is expected from the K content. It may be recalled that it is difficult to make stoichiometric $LaMnO_3$ as some of the Mn is oxidized to 4+. Final formula has been given for each composition in table 1.

FT–IR spectra of $La_{1-x}K_xMnO_3$ ($0{\cdot}00 \le x \le 0{\cdot}25$) compounds are shown in figure 5(a–f). The IR spectrum shows two absorption bands around 600 and 400 cm^{-1} for the compositions (a) $x = 0{\cdot}0$, (b) 0·05 and (c) 0·10. The

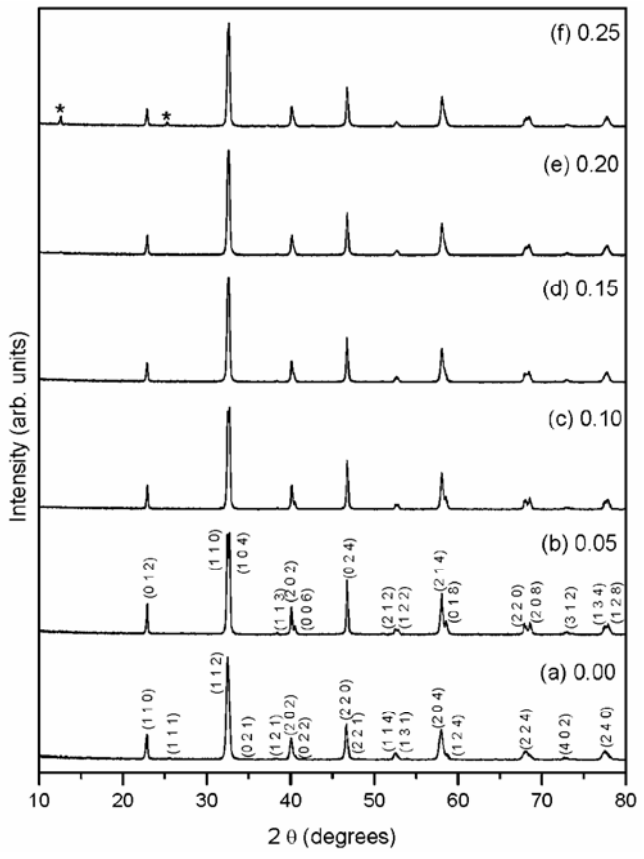

Figure 2. Powder X-ray diffraction patterns of $La_{1-x}K_xMnO_3$ ($0{\cdot}00 \le x \le 0{\cdot}25$) phases, samples sintered at 800°C for 12 h (asterisk indicates layered K_xMnO_2 impurity phase).

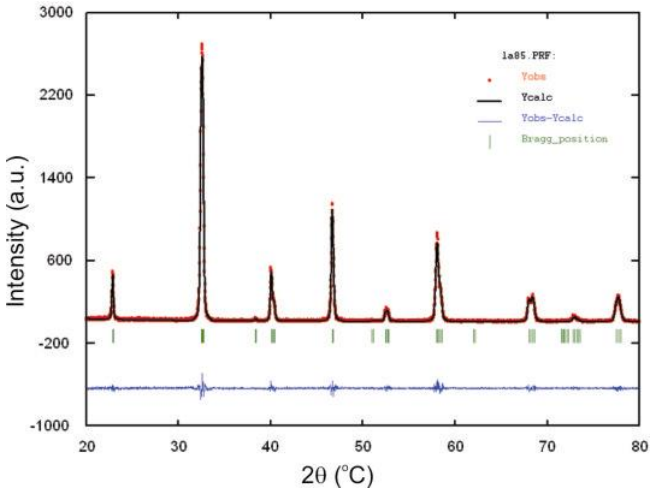

Figure 3. Typical observed, calculated and the difference Rietveld refined X-ray diffraction patterns of $La_{0{\cdot}85}K_{0{\cdot}15}MnO_3$ compound.

Table 1. Rietveld refined structural parameters of $La_{1-x}K_xMnO_3$ ($0 \le x \le 0{\cdot}25$) samples sintered at 800°C for 12 h.

Compounds	$LaMnO_{3{\cdot}07}$	$La_{0{\cdot}95}K_{0{\cdot}05}MnO_{3{\cdot}08}$	$La_{0{\cdot}90}K_{0{\cdot}10}MnO_{3{\cdot}04}$	$La_{0{\cdot}85}K_{0{\cdot}15}MnO_{3{\cdot}01}$	$La_{0{\cdot}80}K_{0{\cdot}20}MnO_{3{\cdot}01}$	$La_{0{\cdot}75}K_{0{\cdot}25}MnO_{2{\cdot}98}$
Lattice parameters						
a (Å)	5·477(6)	5·513(4)	5·511(5)	5·511(4)	5·509(5)	5·506(3)
b (Å)	5·524(4)					
c (Å)	7·805(6)	13·365(8)	13·392(6)	13·391(5)	13·393(2)	13·385(8)
La/Na	(4*e*)	(6*a*)	(6*a*)	(6*a*)	(6*a*)	(6*a*)
x	0·005(12)	0·0000	0·0000	0·0000	0·0000	0·0000
y	0·0120(5)	0·0000	0·0000	0·0000	0·0000	0·0000
z	0·2500	0·2500	0·2500	0·2500	0·2500	0·2500
Mn	(4*b*)	(6*b*)	(6*b*)	(6*b*)	(6*b*)	(6*b*)
x	0·5000	0·0000	0·0000	0·0000	0·0000	0·0000
y	0·0000	0·0000	0·0000	0·0000	0·0000	0·0000
z	0·0000	0·0000	0·0000	0·0000	0·0000	0·0000
O1	(4*e*)	(18*e*)	(18*e*)	(18*e*)	(18*e*)	(18*e*)
x	0·0109(7)	0·4541(3)	0·4621(2)	0·455(6)	0·4613(2)	0·4644(4)
y	0·4869(6)	0·0000	0·0000	0·0000	0·0000	0·0000
z	0·2500	0·2500	0·2500	0·2500	0·2500	0·2500
O2	(8*d*)					
x	0·7500(8)					
y	0·2803(6)					
z	0·0675(3)					
R-factors (%)						
R_P	0·123	0·041	0·073	0·073	0·069	0·079
R_{Bragg}	0·048	0·018	0·015	0·015	0·017	0·018
R_F	0·046	0·019	0·017	0·017	0·016	0·020

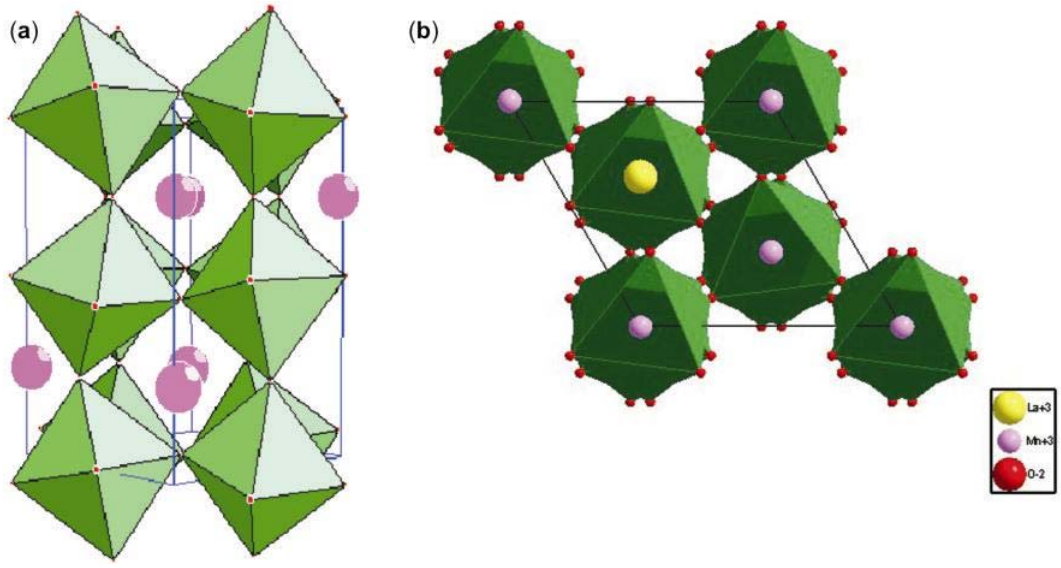

Figure 4. Crystal structures of (**a**) parent $LaMnO_3$ in the orthorhombic and (**b**) $La_{0{\cdot}85}K_{0{\cdot}15}MnO_3$ compound in the rhombohedral structures.

higher frequency band at 600 cm^{-1} was assigned to the Mn–O stretching vibration (ν_s) mode, which involves the internal motion of a change in Mn–O bond length, the band around 400 cm^{-1} corresponds to the bending (ν_b) mode, which is sensitive to a change in the Mn–O–Mn bond angle. These two bands are related to the environment surrounding the MnO_6 octahedra in the ABO_3 perovskite (Arulraj and Rao 1999; Gao *et al* 2002). These absorptions disappear when x exceeds 0·15, on account of the metallic nature of the oxides (figures 5(d–f)).

In figure 6, we showed the resistivity as a function of temperature plots of $La_{1-x}K_xMnO_3$ ($0{\cdot}00 \le x \le 0{\cdot}25$) samples. Parent $LaMnO_3$ compound shows highly insulating behaviour, resistivity value is in the order of 300 KΩ cm at 160 K, when increase in K-content, resistivity value drastically decreased to 5 Ω cm and metal to insulator transition (T_{M-I}) value also shifts to nearly room temperature (287 K) for the composition, $La_{0{\cdot}85}K_{0{\cdot}15}MnO_3$. The resistivity plots reveal that there is a composition-controlled metal to insulator transition in K-substituted $LaMnO_3$ system. The T_{M-I} values observed in the present study were 148, 220, 287, 285 and 280 K for the compositions, x = 0·05, 0·10, 0·15, 0·20 and 0·25, respectively. Generally, solid state preparations yield a bigger grain size and exhibit sharp metal insulator transitions. However, in the present study, all the samples show a broad metal insulator transition and we attribute this to the nano crystalline nature of the grains and weak grain boundary

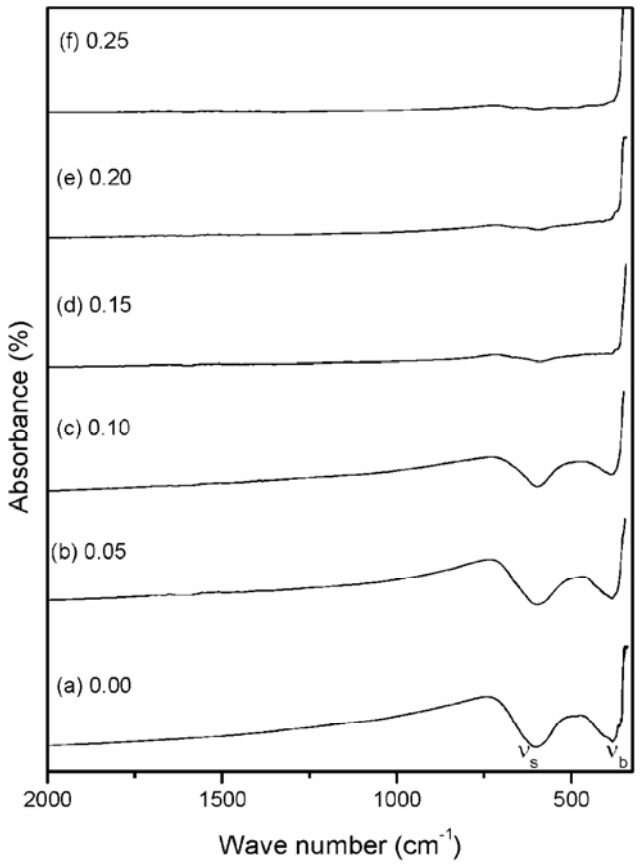

Figure 5. FTIR spectra of $La_{1-x}K_xMnO_3$ ($0{\cdot}00 \le x \le 0{\cdot}25$) compounds sintered at 800°C for 12 h.

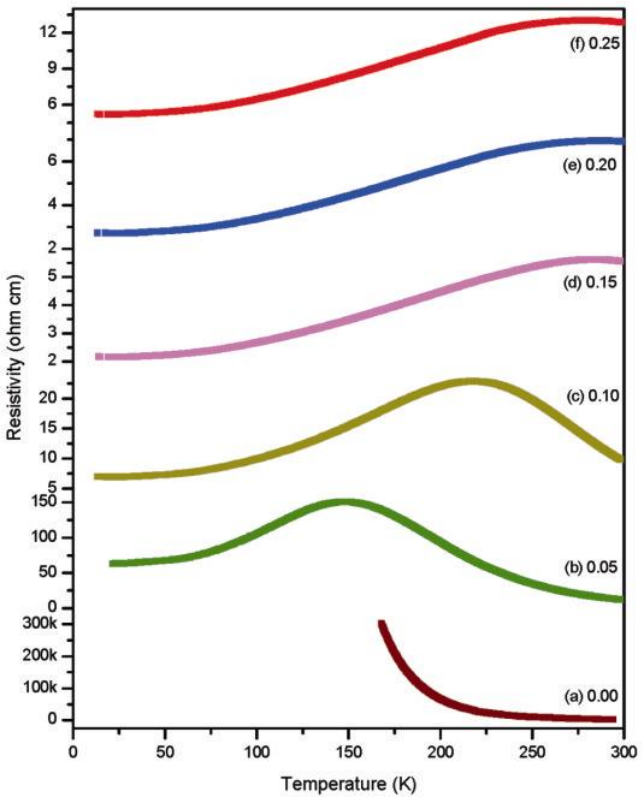

Figure 6. Plots of electrical resistivity as a function of temperature for $La_{1-x}K_xMnO_3$ ($0{\cdot}0 \le x \le 0{\cdot}25$) compounds, pellets sintered at 800°C for 12 h.

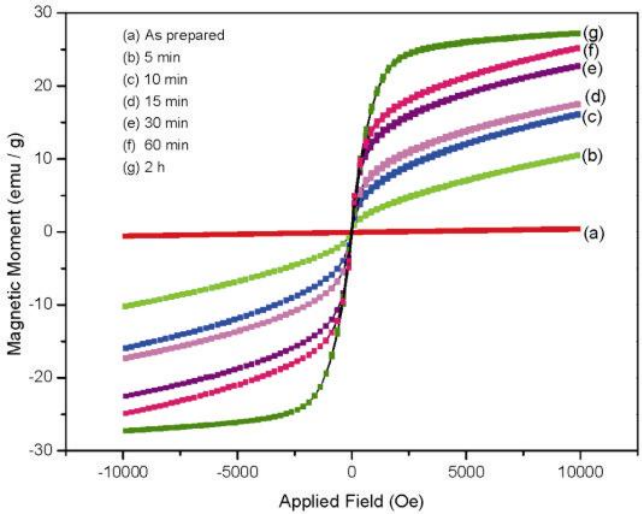

Figure 7. Plots of magnetic moment as a function of applied field for $La_{0{\cdot}85}K_{0{\cdot}15}MnO_3$ compounds calcined at 800°C from 5 min to 2 h.

contact. The effect of grain size on magnetic, transport and structural properties of manganites have been extensively studied by many investigators (Mahendiran *et al* 1996; Hueso *et al* 1998; Wang *et al* 2001; Yang *et al* 2004). These studies suggest that particle size, the doping level in the lanthanum site as well as oxygen content play an important role in the transport properties of these classes of oxides.

In figure 7(a–g), we have shown the magnetic moment as a function of applied field for $La_{0.85}K_{0.15}MnO_3$ compound calcined at 800°C for different times from 5 min to 2 h. In the present work as synthesized sample is not a perovskite phase, therefore, we did not see any ferromagnetism in the sample. On increasing calcinations time from 5 min to 2 h, the magnetic moment also increased. As can be seen from the plot in figure 7(g), the compound heated for 2 h saturated around 2·5 K Oe and exhibit magnetic moment of 27 emu/g.

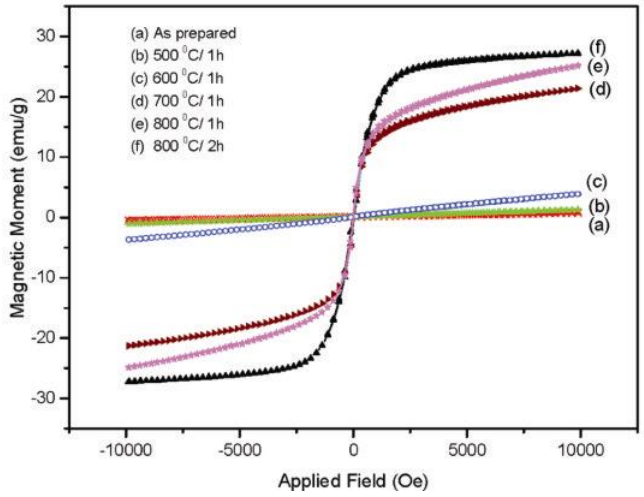

Figure 8. Plots of magnetic moment as a function of applied field for $La_{0.85}K_{0.15}MnO_3$ compounds calcined at different temperatures from 500–800°C for 1 h.

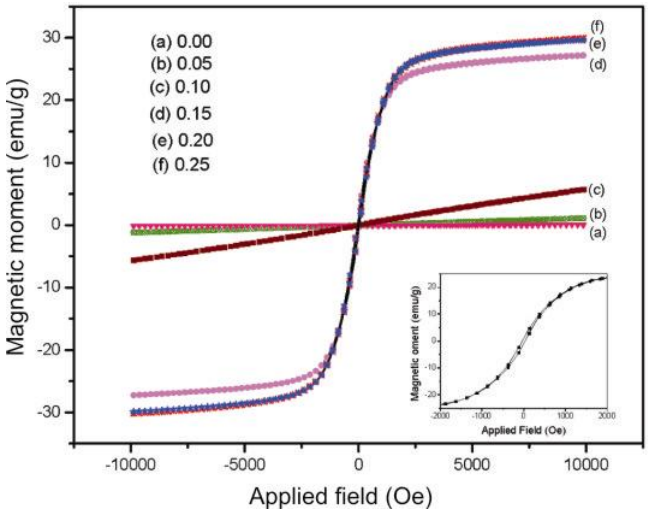

Figure 9. Plots of magnetic moment as a function of applied field for $La_{1-x}K_xMnO_3$ ($0{\cdot}00 \le x \le 0{\cdot}25$) compounds sintered at 800°C for 12 h. In the inset, typical hysteresis loop of $La_{0.85}K_{0.15}MnO_3$ compound is shown.

Further, we performed the magnetization measurement for $La_{0.85}K_{0.15}MnO_3$ samples calcined at different temperatures from 500–800°C for a fixed duration of 1 h, as shown in figure 8(a–e). From figure 8, it is clear that, samples heated up to 600°C for 1 h did not show any magnetic saturation up to 10 K Oe, whereas 700 and 800°C calcined samples did show magnetic saturation. This indicates, compounds crystallized in the perovskite phase at as low as 500°C, in order to get ferromagnetic ordering we have to heat the sample at a minimum temperature of 700°C for 1 h. Figures 7 and 8 clearly demonstrate calcinations time and temperature playing an important role in getting magnetic ordering rather than structural order.

Figure 9 shows magnetization as a function of applied field for $La_{1-x}K_xMnO_3$ ($0{\cdot}00 \le x \le 0{\cdot}25$) compounds sintered at 800°C for 12 h. For the compositions (a) $x = 0{\cdot}00$, (b) 0·05 and (c) 0·10 exhibit paramagnetic like behaviours, there is no magnetic saturation up to 10 K Oe. On the other hand, as the potassium content increases from (d) 0·15, (e) 0·20 and (f) 0·25, compounds are saturated below 2 K Oe and exhibits ferromagnetic properties with magnetic moments of 27, 29 and 30 emu/g, respectively. In the inset, the figure shows typical hysteresis loop of the $La_{0.85}K_{0.15}MnO_3$ compound and it also shows that there is no appreciable change in the hysteresis loop; this reveals that K-substituted $LaMnO_3$ compounds behave like soft magnetic materials.

4. Conclusions

In conclusion, we have shown K-ion can be substituted for La-site in $LaMnO_3$ system by the rapid solution combustion method at relatively low temperature. The structural ordering temperature is as low as 500°C as well as a shorter duration of 5 min at 800°C. On increasing the potassium content, structural transition was observed from orthorhombic to rhombohedral, and composition controlled metal to insulator transition as well as para to ferromagnetic interaction was observed. XRD and VSM data reveals that structural ordering precedes magnetic ordering. Calcination time and temperature play an important role in determining the magnetic ordering.

Acknowledgements

We thank the Department of Science and Technology (FIST–DST), Government of India, New Delhi, for providing XRD, VSM facilities and support to carry out this work. Special thanks are due to Prof. M S Hegde, Solid State and Structural Chemistry Unit, Indian Institute of

Science, Bangalore, for useful discussion and encouragement.

References

Arulraj A and Rao C N R 1999 *J. Solid State Chem.* **145** 557

Aruna S T, Muthuraman M and Patil K C 1997 *J. Mater. Chem.* **7** 2499

Chen C C and de Lozanne A 1997 *Appl. Phys. Lett.* **71** 1424

Gao F, Lewis R A, Wang X L and Dou S X 2002 *J. Alloys & Compd.* **347** 314

Hueso L E, Rivadulla F, Sanchez R D, Caeiro D, Jardon C, Vazquez-Vazquez C, Rivas J and Lopez-Quintela M A 1998 *J. Magn. Magn. Mater.* **189** 321

Itoh M, Shimura T, Yu J D, Hayashi T and Inaguma Y 1995 *Phys. Rev.* **B52** 12522

Jonker G H and Van Santen J H 1950 *Physica* **16** 337

McCarroll W H, Fawcett I D, Greenblatt M and Ramanujachary K V 1999 *J. Solid State Chem.* **146** 88

Mahendiran R, Mahesh R, Raychaudhuri A K and Rao C N R 1996 *Solid State Commun.* **99** 149

Malavasi L, Mozzati M C, Polizzi S, Azzoni C B and Flor G 2003 *Chem. Mater.* **15** 5036

Nagabhushana B M, Chandrappa G T, Sreekanth Chakradhar R P, Ramesh K P and Shivakumara C 2005 *Solid State Commun.* **136** 427

Nagabhushana B M**,** Sreekanth Chakradhar R P, Ramesh K P, Shivakumara C and Chandrappa G T 2006 *Mater. Res. Bull.* **41** 1735

Ng-Lee Y, Safina F, Martinez-Tamayo E, Folgado J V, Ibanez R, Beltran D, Lloret F and Segura A 1997 *J. Mater. Chem.* **7** 1905

Patil K C 1993 *Bull. Mater. Sci.* **16** 533

Patil K C, Aruna S T and Ekambaram S 1997 *Curr. Opin. Solid State and Mater. Sci.* **2** 158

Rao C N R, Cheetham A K and Mahesh R 1996 *Chem. Mater.* **8** 2421

Rao C N R 2000 *J. Phys. Chem.* **B104** 5877

Raveau B, Maignan A, Martin C and Hervieu M 1998 *Chem. Mater.* **10** 2641

Sahana M, Singh R N, Shivakumara C, Vasanthacharya N Y, Hegde M S, Subramanian S, Prasad V and Subramanyam S V 1997 *Appl. Phys. Lett.* **70** 2909

Scherrer 1918 *Nachr. Ges. Wiss. Gottingen, Math.-Phys.* **2** 98

Shannon R D 1976 *Acta Crystallogr.* **A32** 751

Shimura T, Hayashi T, Inaguma Y and Itoh M 1996 *J. Solid State Chem.* **124** 250

Shivakumara C, Subbanna G N, Lalla N P and Hegde M S 2004 *Mater. Res. Bull.* **39** 71

Shivakumara C, Bellakki M B, Prakash A S and Vasanthacharya N Y 2007 *J. Am. Ceram. Soc.* **90** 3852

Singh R N, Shivakumara C, Vasanthacharya N Y, Subramanian S, Hegde M S, Rajagopal S and Sequeira A 1998 *J. Solid State Chem.* **137** 19

von Helmolt R, Wecker J, Holzapfel B, Schultz L and Samwer K 1993 *Phys. Rev. Lett.* **71** 2331

Wang J, Gu B, Sang H, Ni G and Du Y 2001 *J. Magn. Magn. Mater.* **223** 50

Yang J, Zhao B C, Zhang R L, Ma Y Q, Sheng Z G, Song W H and Sun Y P 2004 *Solid State Commun.* **132** 83